

## ***parachute/n-cadherin* is required for morphogenesis and maintained integrity of the zebrafish neural tube**

Zsolt Lele<sup>1,\*</sup>, Anja Folchert<sup>2,\*</sup>, Miguel Concha<sup>3</sup>, Gerd-Jörg Rauch<sup>4</sup>, Robert Geisler<sup>4</sup>, Frédéric Rosa<sup>5</sup>, Steve W. Wilson<sup>3</sup>, Matthias Hammerschmidt<sup>1,†</sup> and Laure Bally-Cuif<sup>2</sup>

<sup>1</sup>Max-Planck Institute for Immunobiology, Stuebeweg 51, D-79108 Freiburg, Germany

<sup>2</sup>Zebrafish Neurogenetics Junior Research Group, Institute of Virology, Technical University-Munich, Trogerstrasse 4b, D-81675 Munich, Germany and GSF-National Research Center for Environment and Health, Institute of Mammalian Genetics, Ingolstaedter Landstrasse 1, D-85764 Neuherberg, Germany

<sup>3</sup>Department of Anatomy and Developmental Biology, University College London, Gower Street, London WC1E 6BT, UK

<sup>4</sup>Max-Planck Institute for Developmental Biology, Spemannstrasse 35, D-72076 Tübingen, Germany

<sup>5</sup>INSERM U368 Groupe Danio, Ecole Normale Supérieure, 46 rue d'Ulm, 75005 Paris, France

\*These authors contributed equally to the work

†Author for correspondence (e-mail: hammerschmid@immunbio.mpg.de)

Accepted 18 April 2002

### SUMMARY

**N-cadherin (Ncad) is a classical cadherin that is implicated in several aspects of vertebrate embryonic development, including somitogenesis, heart morphogenesis, neural tube formation and establishment of left-right asymmetry. However, genetic in vivo analyses of its role during neural development have been rather limited. We report the isolation and characterization of the zebrafish *parachute* (*pac*) mutations. By mapping and candidate gene analysis, we demonstrate that *pac* corresponds to a zebrafish *n-cadherin* (*ncad*) homolog. Three mutant alleles were sequenced and each is likely to encode a non-functional Ncad protein. All result in a similar neural tube phenotype that is most prominent in the midbrain, hindbrain and the posterior spinal cord. Neuroectodermal cell adhesion is**

**altered, and convergent cell movements during neurulation are severely compromised. In addition, many neurons become progressively displaced along the dorsoventral and the anteroposterior axes. At the cellular level, loss of Ncad affects  $\beta$ -catenin stabilization/localization and causes mispositioned and increased mitoses in the dorsal midbrain and hindbrain, a phenotype later correlated with enhanced apoptosis and the appearance of ectopic neurons in these areas. Our results thus highlight novel and crucial in vivo roles for Ncad in the control of cell convergence, maintenance of neuronal positioning and dorsal cell proliferation during vertebrate neural tube development.**

Key words: Zebrafish, Neural tube, *parachute*, N-cadherin

### INTRODUCTION

Cadherins constitute a family of Ca<sup>2+</sup>-dependent cell adhesion molecules crucial for several steps during embryonic development. N-cadherin (cadherin 2, Ncad) belongs to the subfamily of classical cadherins characterized by five extracellular cadherin-binding domains separated by Ca<sup>2+</sup>-binding pockets, a transmembrane domain and an intracellular  $\beta$ -catenin-binding domain (for a review, see Tepass et al., 2000). It was discovered as the first of about 30 cadherins expressed in the vertebrate embryonic or adult nervous system (Hatta and Takeichi, 1986; Miyatani et al., 1989; Redies, 2000; Yagi and Takeichi, 2000). *Ncad* expression is relatively ubiquitous during early vertebrate development, but later becomes restricted to particular sets of nuclei and neuronal layers within the central nervous system (CNS) (Redies et al., 1993; Redies and Takeichi, 1993). *Ncad* mRNA is also expressed in the eyes, in various ganglia of the peripheral nervous system, and in the developing heart and somites.

Most evidence regarding Ncad function has been gathered from cell culture experiments. Forced expression of *Ncad* causes increased migration, invasiveness and metastatic activity in breast cancer cell lines (Hazan et al., 2000; Nieman et al., 1999). Accordingly, upregulation of *Ncad* expression accompanied by loss of *E-cadherin* mRNA is potentially a key event in the epithelial-mesenchymal transitions associated with the metastatic phenotype during cancer progression (Tran et al., 1999). Moreover, ectopic expression of *Ncad* is also reported to induce scattering and epithelial-mesenchymal transition in squamous carcinoma cells (Islam et al., 1996), as well as reduced adhesion and increased migration in oligodendrocyte cultures on astrocyte monolayers (Schnadelbach et al., 2000). In contrast to these results, increased attachment and reduced motility has been observed following overexpression of *Ncad* in murine sarcoma cells (Dufour et al., 1999). These apparently contradicting results demonstrate that Ncad may regulate cell adhesion and migration in a tissue- and context-specific manner.

To date, the *in vivo* functions of Ncad during vertebrate embryonic development have been studied in knockout mice and in manipulated chick and *Xenopus* embryos. *Cdh2*<sup>-/-</sup> (Mouse Genome Informatics) mice possess an undulating neural tube, undifferentiated somites and severe cardiac defects. The cardiac defects, which are due to impaired cardiomyocyte differentiation, cause early embryonic death (Radice et al., 1997), thereby making it impossible to study later, essential functions of Ncad. Recently, however, this problem was overcome by rescuing the heart phenotype with cardiac-specific expression of *Cdh2* in the knockout mouse (Luo et al., 2001). Such embryos are characterized by a morphologically malformed neural tube and by increased apoptosis in neural and somitic tissues. The role of Ncad during somitogenesis has been further elucidated using Ncad-blocking antibodies on cultures of mouse and chick paraxial mesoderm. These treatments caused the formation of small ectopic somites in lateral positions, probably as a result of excess segmentation of the original presomitic mesoderm (Linask et al., 1998). Thus, Ncad function is important for the ordered segmentation of the paraxial mesoderm. When applied on chick embryos cultured from an earlier stage, Ncad antibodies also cause situs inversus, implicating Ncad in the control of left-right asymmetry in this system (Garcia-Castro et al., 2000). However, the neural phenotype of Ncad-deficient mouse or chick embryos has not been analyzed in detail. Function-blocking experiments, using Ncad-specific antibody or a dominant negative version of Ncad, injected in the tectal and hindbrain ventricles, respectively, caused loss of neuroepithelial structure and prevented delamination of melanocyte precursor neural crest cells (Gänzler-Odenthal and Redies, 1998; Nakagawa and Takeichi, 1998). These approaches, however, only produce local effects and their specificity is difficult to ascertain.

We describe three alleles of the zebrafish *parachute* (*pac*) mutant which carry potential null mutations in a zebrafish *ncad* homolog (*cdh2* – Zebrafish Information Network). In contrast to *Cdh2*-deficient mice, *pac* mutants most strongly suffer from impaired neural tube development, particularly in the midbrain and hindbrain. We provide a detailed analysis of this phenotype highlighting new and critical roles for Ncad in the control neural tube development. A possible connection between Ncad and  $\beta$ -catenin function during neural tube development is discussed.

## MATERIALS AND METHODS

### Bodipy-ceramide staining and confocal microscopy

Bodipy-ceramide (Fl C5, Molecular Probes) was dissolved in DMSO to a stock concentration of 5 mM. Dechorionated embryos were soaked in 100  $\mu$ M bodipy-ceramide solution for 30 minutes in the dark. The embryos were then washed and embedded in low-melting point agarose for confocal microscopy.

### Cell transplantations

Donor embryos were injected with 1% biotin-1% rhodamine dextran or with 40 ng/ $\mu$ l capped GFP mRNA at the 1- to 4-cell stage. Cell transplantations were carried out as previously described (Ho and Kane, 1990), with recipient and donor embryos maintained in the dark at all stages. The appropriate localization of transplanted cells was checked under fluorescent light, and the recipient embryos were fixed

at 24 hours of development. For single labeling, biotin-dextran was revealed using the ABC-HRP kit (Vectastain). For double labeling, biotin-dextran was detected using streptavidin- $\beta$ -galactosidase (Roche) followed by X-gal staining; GFP protein was revealed by immunocytochemistry using mAb anti-GFP (Quantum) as described (Bally-Cuif et al., 2000). Stained embryos were post-fixed, embedded in JB4 resin (Polysciences) and sectioned at 7  $\mu$ m with an ultramicrotome.

### Mapping of *pac*

*pac*<sup>tm101</sup> was mapped by crossing a Tü mutant carrier with a WIK reference (Rauch et al., 1997) and collecting the F<sub>2</sub> offspring. A set of 240 SSLP markers (Knapik et al., 1996) were then tested on pools of 48 mutants and 48 siblings. Linkages from the pools were confirmed and refined by genotyping single embryos.

### Cloning and sequencing of full-length *ncad*

Full-length cDNA was isolated using gastrula stage total RNA and a RACE-PCR kit (Clontech) according to manufacturers' protocols with primer (5'-GGCGTAACTAGTCGTCGTTACCTCCGTAC-3') made to the 3'-end of the coding region. Full-length cDNA was obtained with the Expand Long Template PCR kit (Roche Biochemicals) in one PCR reaction and cloned into pCR 2.1 vector (Invitrogen). Sequencing of the clones was carried out using gene-specific primers, Big Dye termination mix and ABI-Prism 310 sequencing machine.

### In situ hybridization and immunohistochemistry

Probe synthesis, *in situ* hybridization and immunohistochemistry were carried out as previously described (Hammerschmidt et al., 1996). Acetylated-tubulin antibody was obtained from Sigma, the phosphoHistone3 Ab was from Upstate Biotechnology and the 3A10 Ab from the Developmental Studies Hybridoma Bank, University of Iowa. Rabbit anti- $\beta$ -catenin was purchased from Sigma and used at 1/2000 dilution.  $\beta$ -catenin staining was carried out on 20  $\mu$ m cryostat sections cut from the midbrain level and analyzed via confocal microscopy at 2  $\mu$ m intervals.

### Western blot analysis

Embryonic protein extracts were separated via conventional SDS-PAGE (12% acrylamide:bisacrylamide 38:1), blotted and incubated with the rabbit anti-N-cadherin antibody R851 (Bitzur et al., 1994) at 1/100, followed by a secondary goat anti-rabbit-HRP antibody (Jackson) at 1/2000. Blots were developed with the ECL developing system (Amersham).

### Antisense experiments

Morpholino antisense oligonucleotides (MOs) were purchased from Gene-Tools. MOs were dissolved to a stock concentration of 1mM and injected into 1- to 4-cell stage embryos at the following concentrations (Nasevicius and Ekker, 2000):

*ncad* MO1 (5'-TCTGTATAAAGAAACCGATAGAGTT-3'; corresponds to -40 to -16 of *ncad* cDNA), 50  $\mu$ M;  
*ncad* MO2 (5'-CGGTGAAACCAGGCTGACATGGCAT-3'; corresponds to +72 to +96 of *ncad* cDNA), 100  $\mu$ M; and  
 4mm-MO (5'-TCTcTATAAAcAAACgGATAGtGTT-3'), 50  $\mu$ M.

### Retrograde labeling of reticulospinal neurons

Labeling of reticulospinal neurons was performed as previously described (Moens et al., 1996). Briefly, 4- to 5-day-old embryos were anesthetized in MS222 (Sigma) and immobilized in drops of 1% low melting point agarose in embryo medium. Their lower trunk and tail was then sectioned using a fine blade previously soaked into 5% fixable rhodamine dextran (Molecular Probes). After a few minutes, the embryos were returned to fresh medium, allowed to recover for 1 hour, and fixed overnight at 4°C in 4% paraformaldehyde. The brains were dissected out using fine forceps, mounted in 80% glycerol in

PBS and analyzed under fluorescence with a Zeiss Axioplan photomicroscope.

### Uncaging experiments

A solution of 10 kDa DMNB-caged fluorescein (5 mg/ml; Molecular probes) was injected into 1-cell embryos, which were allowed to develop further in the dark. At the shield-60% epiboly stage, the dye was activated in a single blastomere using a microlaser beam (Photonics Instruments) (Serbedzija et al., 1998). The irradiated blastomere was chosen 5- to 6-cell rows lateral to the axial midline at the anteroposterior level of the notochord tip, according to the extrapolated position of the ventral midline domain of the mid- and hindbrain presumptive territories (Woo and Fraser, 1995). At the 20-somite stage, irradiated embryos were fixed overnight in 4% paraformaldehyde at 4°C and processed for anti-fluorescein immunocytochemistry (Dickmeis et al., 2001).

## RESULTS

### Isolation and morphology of *parachute* (*pac*) mutants

In two independent screens (Z. L., T. Mayr and M. H., unpublished; F. R., unpublished), we isolated two new ENU-induced mutations causing phenotypes similar to those previously reported for *parachute* (*pac*) mutants (Jiang et al., 1996). Complementation crosses between the new mutants and the *pac* allele *tm101B* produced one quarter of embryos (134/507=26.4%; 173/682=25.4%, respectively) indistinguishable from *pac<sup>tm101B</sup>* mutants (Jiang et al., 1996). Therefore, the two new mutations were named *pac<sup>fr7</sup>* and *pac<sup>paR2.10</sup>*.

Homozygous *pac<sup>fr7</sup>* and *pac<sup>paR2.10</sup>* embryos display a very similar neural phenotype. Mutant embryos are first recognizable at the eight-somite stage when in optical cross-section the hindbrain appears mushroom shaped rather than oval (Fig. 1A,B). By 24 hours after fertilization (hpf), the phenotype is most obvious at the midbrain-hindbrain region and in the tail (Fig. 1C,D). The midbrain and hindbrain appear generally disorganized with no morphologically distinct midbrain-hindbrain boundary (Fig. 1E,F), and an enlarged fourth ventricle extending into the midbrain. In addition, cell aggregates, detached from the neuroepithelium, were observed in the ventricle. In the tail, the caudal-most part of the dorsal finfold is reduced, less erect and often split along the midline (Fig. 1G-I).

### The *pac* mutation affects the adhesiveness of neuroectodermal cells

Our gross phenotypical analysis suggests that *pac* might affect cell adhesion processes during neural tube development. To confirm this hypothesis at the cellular level, we carried out bodipy-ceramide staining and cell transplantation experiments to visualize cell interactions. Bodipy-ceramide labeling outlines cell contours and reveals the polarized and elongated epithelial structure of cells in the wild-type hindbrain (Fig. 2A). In *pac* mutant embryos, neuroepithelial cell organization in the ventral (basal) part of the neural tube appears normal, whereas dorsal (alar) cells are frequently more rounded and are present in aggregates separated by large intercellular spaces (Fig. 2B). These aggregates often organize into rosettes that appear to cavitate and enclose a central lumen (Fig. 2C). This

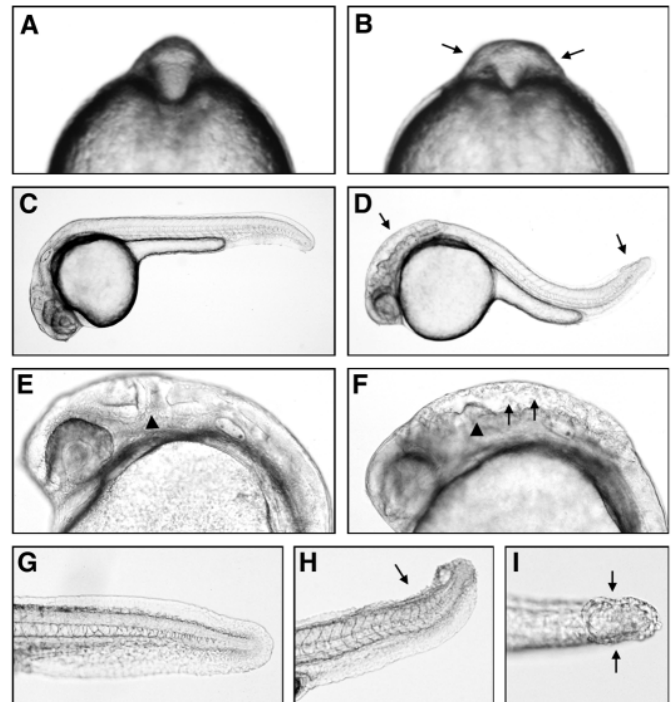


**Fig. 1.** *pac* mutants exhibit abnormal brain and tail morphogenesis. (A,C,E,G) Wild-type siblings, (B,D,F,H,I) *pac<sup>fr7</sup>* mutants. (A,B) Eight-somite stage, frontal view, arrows in B indicate broadened neural tube at midbrain-hindbrain level. (C-I) 24 hpf. (C,D) lateral overview; arrows in D indicate sites of phenotypic defects in the midbrain-hindbrain region and tip of tail. (E,F) Magnification of head region; arrowheads in E,F indicates the position of the midbrain-hindbrain boundary, arrows in F indicate loose cell aggregates in ventricle. (G-I) Magnification of tip of tail; lateral view (G,H) and dorsal view (I); arrows in H,I indicate region with split dorsal fin.

suggests that some degree of neuroepithelial cell polarity may be retained in *pac* mutants, but that dorsal neural cells lose the adhesive interactions required for the formation and/or maintenance of a normal neural tube structure.

To provide direct evidence for the altered adhesiveness of *pac* neuroectodermal cells, we analyzed cell morphology in the neural tube of *pac<sup>fr7</sup>*/wild-type chimeric embryos generated via cell transplantations. We first verified that wild-type cells transplanted into a wild-type host always acquired a normal elongate neuroepithelial appearance in both the basal and the alar plates (Fig. 2D,G; 60/60). Furthermore, as in *pac* mutants (Fig. 2B,C), *pac* cells transplanted into a *pac* host possessed neuroepithelial morphology in the basal plate, but were disorganized in the alar plate (Fig. 2H; 7/7). These observations indicate that cell distribution and morphology are not biased by our transplantation procedure compared with the endogenous situation of wild-type or mutant embryos. When transplanted to a *pac<sup>fr7</sup>* mutant host, however, wild-type cells formed tight aggregates that did not mix with surrounding mutant cells (Fig. 2E,I; 29/29). Only occasionally, isolated wild-type cells were observed in the (morphologically unaffected) basal regions of the *pac* hosts. They were integrated into the neuroepithelium and displayed elongate morphology (Fig. 2J). In the reverse transplantation of *pac*

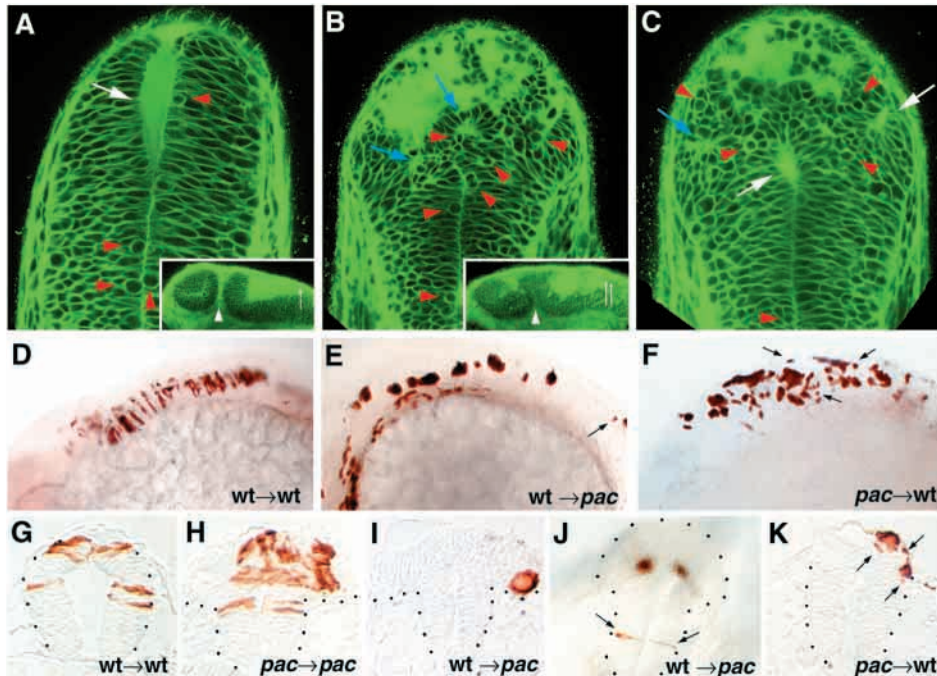


**Fig. 2.** The *pac* mutation affects cell-cell adhesion in the midbrain-hindbrain region. (A-C) Bodipy ceramide staining; 24 hpf; confocal microscopic cross sections at hindbrain levels; (A) wild-type sibling, (B,C) *pac*<sup>fr7</sup> mutant. Red arrowheads indicate rounded cells, blue arrows indicate ectopic rosette-like structures in dorsal regions of the *pac* mutant, and white arrows indicate ventricle lumen of the neural tube and ectopic lumina in dorsal rosette-like structures in *pac*. Insets in A,B show longitudinal sections through the mid- and hindbrain. The midbrain-hindbrain boundary (mhb) is indicated by white arrowheads and levels at which the cross-sections are taken are indicated by white arrows. Note the less pronounced mhb in *pac* mutant (B). (D-K) Chimeric embryos after transplantation of wild-type or *pac* mutant cells into wild-type or *pac* mutant hosts, as indicated; 24 hpf; lateral view of the mid- and hindbrain (D-F) and transverse sections at midbrain-hindbrain level (G-K). Note the tighter organization of the aggregate in I compared with K. Arrows in E,F,J,K indicate isolated cells. Note that in K, isolated *pac* mutant cells have a rounded shape, in contrast to their elongated wild-type neighbors (compare with alar wild-type cells in G).

mutant cells into wild-type hosts, mutant cells always ended up in alar regions of the neural tube (Fig. 2K; 24/24; see also below). Mutant cells also tended to aggregate, however, these aggregates appeared much looser than the aggregates of wild-type cells in *pac* mutants (compare Fig. 2I with 2K), and isolated donor cells occurred at a much higher rate than in wild-type/*pac* chimeras (compare Fig. 2E with 2F). These isolated *pac* mutant cells always showed rounded morphology, despite the neuroepithelial organization of their wild-type neighbors (Fig. 2K). Together, these results demonstrate that the *pac* mutation affects cell adhesiveness, causing defects in cell morphology and cell-cell interactions, which are most prominent in alar regions of the neural tube.

#### *pac* encodes zebrafish *ncad*

To map the *pac*<sup>tm101B</sup> mutation, homozygous F<sub>2</sub> mutants from a Tü/wik linkage cross were tested for the selected panel of SSLP markers (G.-J. R. and R. G., unpublished). Results obtained using genomic DNA from embryo pools and, subsequently, from single embryos put *pac* on LG 20, in close proximity to the SSLP marker z3964 (no recombination in 113 embryos=226 meiosis; see Fig. 3A). Searching for genes and ESTs that map to this region, we found *cadherin 2 (ncad)*

(Bitzur et al., 1994). This gene was a good candidate, given previous work suggesting putative roles for *ncad* orthologs in mediating cell-cell interactions. *ncad* expression starts at late blastula stages, and persists during gastrula and segmentation stages. The early expression is rather ubiquitous, only becoming restricted to the CNS from around 24 hpf (Fig. 3C-F) (Bitzur et al., 1994).

RT-PCR analyses of *ncad* transcripts from single and pooled *pac*<sup>paR2.10</sup> mutant embryos in comparison to wild-type embryos (using the absence of the wild-type *ncad* cDNA as the genotyping criterion; see below; Fig. 3G) revealed no recombination in 110 meioses, indicating that the *pac*<sup>paR2.10</sup> mutation and the *ncad* gene are closely linked and within 0.9 cM.

Based on these findings, we proceeded to clone and sequence *ncad* cDNA from three different *pac* alleles. We first cloned full-length *ncad* cDNA, as the earlier published protein sequence (Bitzur et al., 1994) lacked ~100 N-terminal amino acids compared with Ncad proteins from other vertebrates. Via 5' RACE-PCR, we isolated a 2878 bp cDNA clone with a 2683 bp open reading frame encoding a protein of 893 amino acids, 111 amino acids longer than the previously reported zebrafish Ncad sequence. The protein contains an N-terminal signal sequence (confirmed

by running sequence through SMART), and the cDNA has an in frame upstream stop codon, indicating that the clone is full length (GenBank Accession Number AF418565).

Sequencing *ncad* cDNA from *pac*<sup>tm101B</sup> and *pac*<sup>fr7</sup> alleles revealed point mutations that introduce premature stop codons into the coding region. Interestingly, the stop codons of both alleles are only 13 amino acids apart. In the *pac*<sup>fr7</sup> allele, a TCG →TAG exchange leads to a Ser →Stop at amino acid 501 in the Ca<sup>2+</sup>-binding pocket between extracellular cadherin-binding (EC) domains 3 and 4, while in *pac*<sup>tm101B</sup>, Tyr514 at the beginning of EC domain 4 is converted to Stop due to a TAT →TAA nonsense mutation (Fig. 3B).

In contrast to *pac*<sup>tm101B</sup> and *pac*<sup>fr7</sup>, RT-PCR amplification of *ncad* mRNAs from *pac*<sup>paR2.10</sup> mutants failed to amplify a transcript of wild-type size. Rather, one smaller and three larger transcripts were generated (Fig. 3G), most likely as a result of incorrect splicing of the precursor mRNA. The short transcript (Fig. 3G, transcript S) has a 130 nt deletion from -72 to +48 of the wild-type cDNA, including the start codon. The deleted sequence starts with GT and ends with AG, the consensus sequences of intron borders. The three longer transcripts (Fig. 3G; transcripts L1,2,3) carry insertions with identical 5' sequences, but variable 3' extensions, at position

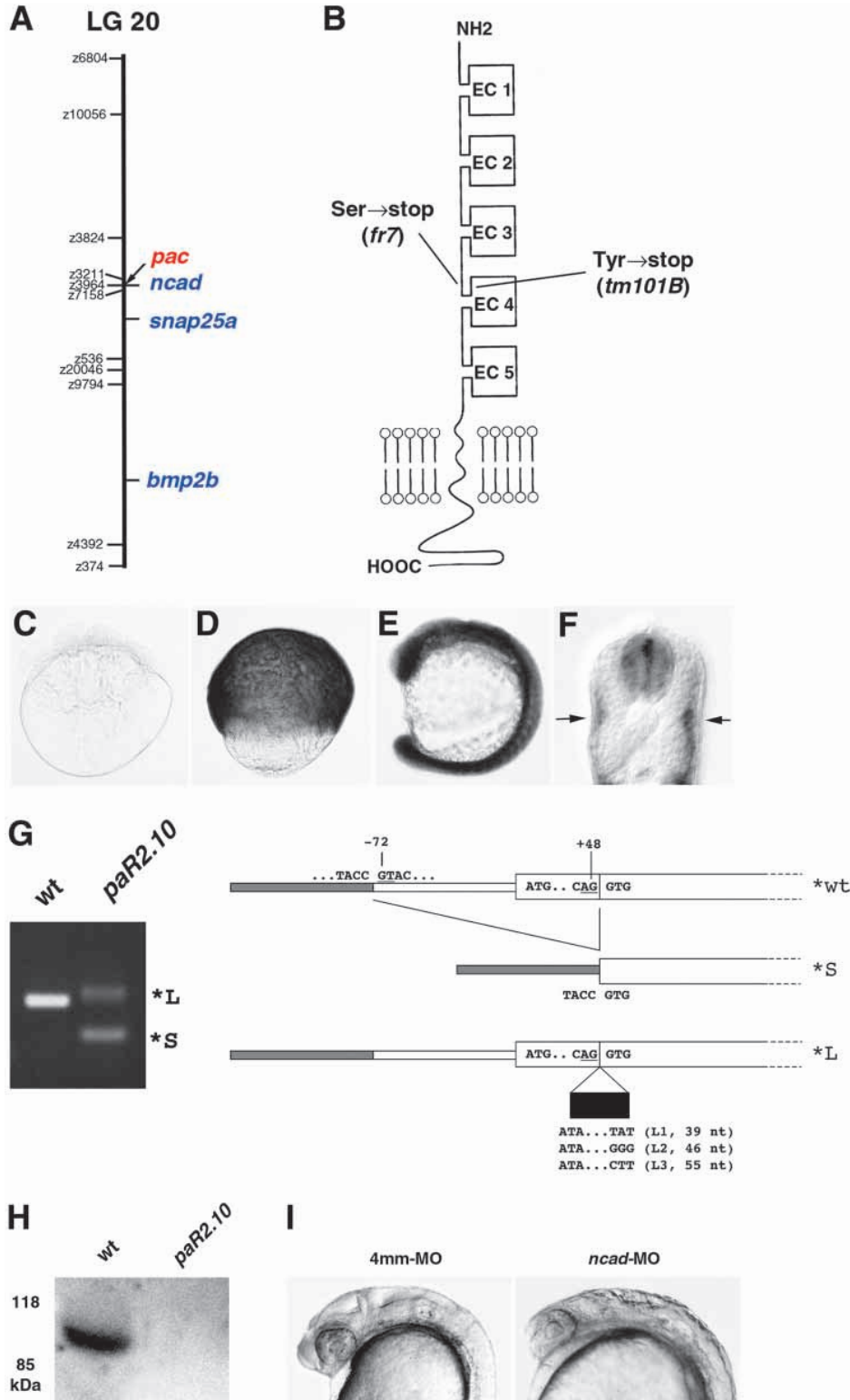


**Fig. 3.** *pac* encodes N-cadherin. Map positions of the *pac<sup>tm101B</sup>* mutation and the *ncad* gene on linkage group 20. Cartoon of the structure of Ncad protein. As indicated, Ncad encoded by *pac<sup>tm101B</sup>* and *pac<sup>fr7</sup>* displays premature terminations in the extracellular region, shortly after the EC3 domain. (C-F) Expression pattern of *ncad*. (C) Eight-cell stage, lateral view. (D) 80% epiboly stage, lateral view. (E) Fifteen-somite stage, lateral view. (F) 24 hpf, cross-section at trunk level. *ncad* expression is restricted to neural tube and slow muscle fibers. (G) RT-PCR analysis of *ncad* transcripts from *pac<sup>paR2.10</sup>* mutants, and structure of their 5' regions. From *pac<sup>paR2.10</sup>* RNA, no wild-type, but only a predominant smaller transcript (\*S) and different larger *ncad* transcripts (\*L) were amplified. (H) Western blot analysis of protein extracts from a *pac<sup>paR2.10</sup>* and a wild-type sibling embryo with a polyclonal antibody against EC domains 4,5 of zebrafish Ncad (Bitzur et al., 1994). The wild-type extract gives an Ncad-positive band of the expected size, whereas no such band is seen in extracts from the *pac<sup>paR2.10</sup>* mutant. Before antibody incubation, the blot had been stained with Ponceau Red, showing that equal amounts of proteins were loaded in both lanes. Similar analyses failed to detect Ncad protein from *pac<sup>fr7</sup>* mutants, as expected, because, according to the cDNA sequence, *pac<sup>fr7</sup>* mutant protein terminates after the third EC domain. (I) Phenocopy of the *pac* mutant phenotype with anti-*ncad* morpholino *ncad*-MO1 (right, compare with Fig. 1F) and with the four-mismatch control MO (left) (see Materials and Methods). Embryos at 24 hpf, lateral view of head region.

+48 of the coding region. L1 has a 39 nt insertion (5'-ATAAAACGAAGGGTCCGAGGAGCGATGCTGCTGCTCT-AT-3'), causing an in frame insertion of 13 foreign amino acid residues (aa) into the protein, L2 has a 46 nt insertion (5'-L1+GTTTGGG-3'), causing a frame shift and premature termination of the protein after 35 non-specific aa, and L3 a 55 nt insertion (5'-L2+GTTTGGCTT-3'), causing a frame shift

and premature termination after 38 non-specific aa. The most likely reason for these false transcripts is a G→A mutation in the splice donor site (GT) of an intron inserted at +48. According to this notion, the insertions of the large transcripts (ATAAAA...) represent intron sequences with the mutated splice donor site, so that alternative sites are used as splice donors, such as the GT at -72 (to give the short transcript) or GTs inside the intron, such as the underlined GT in L2 to give L1, or the underlined GT in L3 to give L2. Western blot analysis of protein extracts from single *pac<sup>paR2.10</sup>* embryos with a polyclonal antibody directed against extracellular domains 4 and 5 of zebrafish Ncad (Bitzur et al., 1994), failed to detect any protein (Fig. 3H), suggesting that little or no Ncad protein is made from the *pac<sup>paR2.10</sup>* *ncad* transcripts.

Finally, to support further our finding that *pac* is a mutation

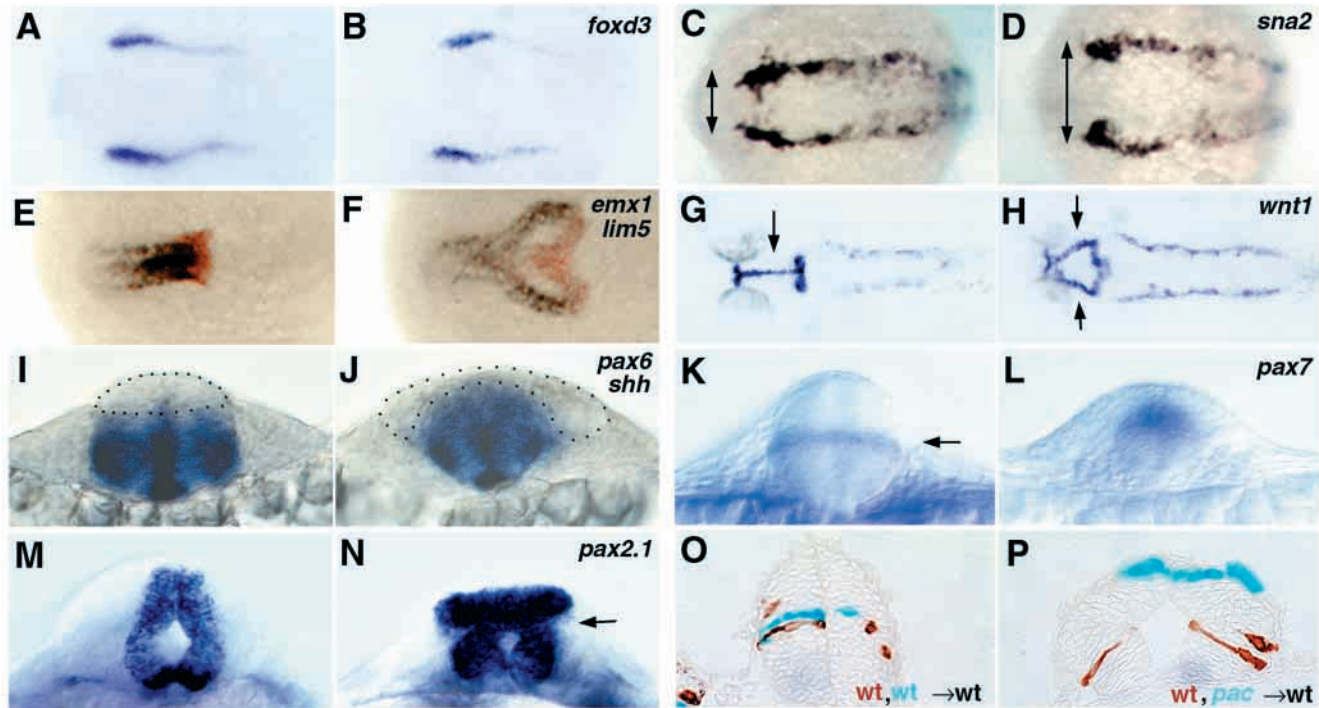


**Fig. 4.** Lack of *Ncad* causes neurulation defects. (A–N) Whole-mount in situ hybridization for the markers indicated in the top right-hand corner. Dorsal views with anterior towards the left in A–H; optical cross sections dorsal upwards in I–N; all paired panels compare a *pac* mutant (right) with a wild-type sibling (left). (O, P) Mid-hindbrain cross-sections of wild-type embryos co-transplanted with cells from two different donors, as indicated in the bottom right-hand corner; donor cells are stained in cyan or brown. (A, B) *foxd3*, three-somite stage; note the identical mediolateral extent of the neural plate in wild-type and *pac*. (C, D) *sna2*, five-somite stage; arrows indicate the width of neural plate delineated by *sna2* stripes, larger in *pac*. (E, F) *emx1* (blue; marking telencephalon) + *lim5* (red; marking posterior diencephalon) (Toyama et al., 1995a), 10-somite stage. In F, cells in the fused part of the *lim5* expression domain are located ventrally, cells in the bilateral parts dorsally. (G, H) *wnt1*, 26 hpf; arrows indicate fused (G) and bilateral (H) expression domains in the midbrain. (I, J) *pax6* + *shh*; 12-somite stage; section at hindbrain level. The alar plate devoid of *pax6* staining is outlined by dots. (K, L) *pax7*, 16-somite stage; optical section at hindbrain level. Arrow in K indicates a *pax7* stripe in the interface of basal and alar plate. (M, N) *pax2.1*, 24 hpf; optical cross-section through midbrain-hindbrain boundary region; arrow indicates the region where basal and alar plate have morphologically separated. (O, P) Chimeric embryos, 24 hpf, cross-section at midbrain (P) and hindbrain (O) levels. Note that in P, wild-type cells (in brown) populate the basal plate, while *pac*<sup>*paR2.10*</sup> mutant cells (in cyan) remain alar, although both cell types had initially been transplanted to the same presumptive basal region of the host embryo.

in the zebrafish *ncad* gene, we phenocopied the *pac* mutant phenotype in wild-type embryos by injecting morpholino antisense oligonucleotides (MOs) targeting two different sequences at the 5' end of the coding region and the 5'UTR of the *ncad* mRNA (see Materials and Methods). MOs have been shown to knock-down efficiently the translation of various genes in zebrafish (Nasevicius and Ekker, 2000) and both *ncad*-MOs phenocopied the *pac* mutation with high accuracy (compare Fig. 3I with Fig. 1F), while a four-mismatch control morpholino (4mm-MO) had no effect (Fig. 3I, left panel).

We conclude that *pac* encodes zebrafish *Ncad*, and that the three *pac* alleles *tm101b*, *fr7* and *paR2.10* are likely to produce null phenotypes.

#### ***ncad* controls neural tube morphogenesis**

As shown above, the first morphological sign of the *pac* mutant phenotype is the different shape of the neural tube, which in cross-section appears dorsally broadened (Fig. 1A, B). Therefore, we considered the possibility that early DV patterning of the prospective neuroectoderm may be disrupted in *pac* mutants. To test this hypothesis, we examined *pac*

mutants from late gastrula to three-somite stages with a range of markers for different DV positions within the neural plate. All such markers were expressed in indistinguishable patterns in wild-type and *pac* mutant embryos (Fig. 4A, B for the neural crest marker *foxd3*, and data not shown), indicating that both early DV patterning and positional specification during primary neurogenesis do not require *Ncad* function.

Defects in *pac* mutants first become apparent after the onset of neurulation. By the five- to six-somite stage, the bilateral stripes of expression of the neural crest markers *foxd3* and *sna2* (Odenthal and Nüsslein-Volhard, 1998; Thisse et al., 1995) are wider apart in mutant than in wild-type embryos (Fig. 4C, D), suggesting that prospective dorsal neural cells are compromised in their ability to converge to the dorsal midline during zebrafish neurulation. This is confirmed by analyses at later stages, which show that the expression domains of dorsal markers fail to fuse in the midline of *pac* mutants. This phenotype is most severe in the posterior diencephalon, midbrain and hindbrain, as evidenced by the expression of *emx1*, which labels dorsal cells of the presumptive forebrain (Morita et al., 1995), and *wnt1*, which labels the prospective roofplate in the midbrain and hindbrain (Kelly and Moon,

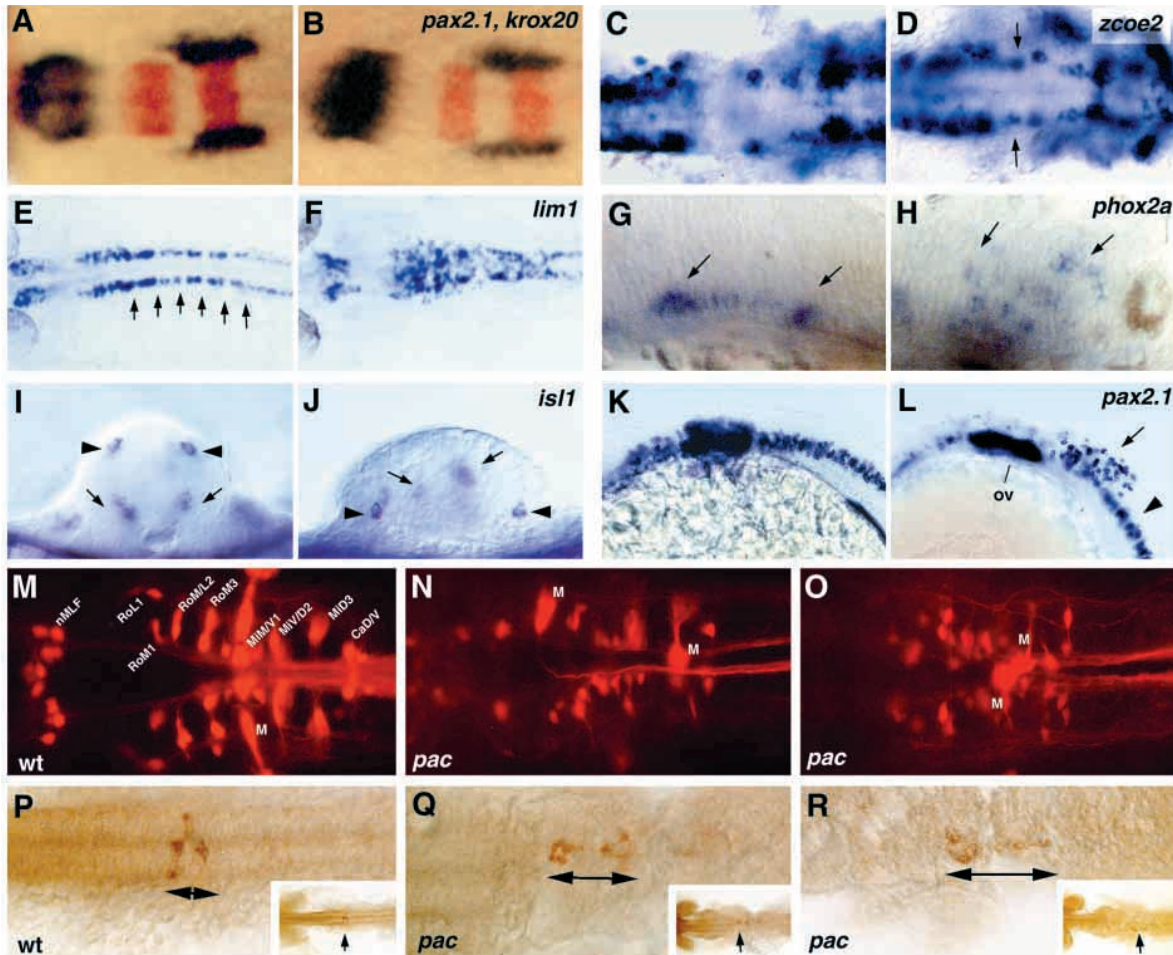


**Fig. 5.** Lack of Ncad causes neuronal positioning defects. In situ hybridization (A-L), retrograde labeling of reticulospinal neurons (M-O) and tracing of cellular clones after labeling single neuroectodermal cells at the gastrula stage (P-R). All paired panels in A-L compare a *pac* mutant (right) with a wild-type sibling (left). (A-F) Dorsal views of the mid- and hindbrain, anterior towards the left; (G,H,K,L) sagittal views of the mid- and hindbrain, anterior towards the left; (I,J) optical cross-sections at hindbrain level, dorsal upwards. (A,B) *pax2.1* (blue) and *krox20* (red), 18-somite stage. (C,D) *zcoe2*, 18-somite stage, arrows in D indicate misplaced motoneurons in the midbrain-hindbrain boundary region. (E,F) *lim1*; 26 hpf; arrows in E indicate the rhombomeric pattern, altered in *pac* (F). In addition, note that the number of *lim1*-positive cells in the mutant is strongly increased. (G,H) *phox2a*, 36 hpf; arrows indicate ventral and dorsally misplaced motoneurons. (I,J) *isl1*, 24 hpf; arrows indicate motoneurons, arrowheads indicate Rohon-Beard sensory neurons. (K,L) *pax2.1*, 26 hpf; arrow in L indicates scattered interneurons in hindbrain area. ov, otic vesicle. (M-N) Pattern of reticulospinal neurons (specified in M) in wild-type (M) and two different *pac*<sup>paR2.10</sup> mutant embryos (N,O; Mauthner neurons are indicated by 'M'); dorsal view on midbrain-hindbrain region at 120 hpf. Patterns in mutants appear randomized, and differ from individual to individual. Although each labeling is unlikely to label all reticulospinal neurons, the patterns observed clearly lack bilateral symmetry at least for the Mauthner neuron (identified by its characteristic elongated shape and large diameter axon, out of focus on O). (P-R) Representative clones (brown) deriving from labeled single cell of the hindbrain region of a wild-type (P) and two *pac*<sup>paR2.10</sup> mutant gastrulae (Q,R). Dorsal view of the hindbrain at 24 hpf. Arrows indicate the length of the clones along AP axis. Insets show overviews of the activated embryos, indicating the position of the clones in each embryo (arrows).

1995; Krauss et al., 1992). Both the *emx1* and the *wnt1* expression domains are fused anteriorly, but remain as separate bilateral stripes within the diencephalon and the mid- and hindbrain of *pac* mutants (Fig. 4E-H) A similar incomplete fusion of dorsal regions of the neural tube is also observed in the posterior part of the tail (not shown), a defect that might underlie the split appearance of the dorsal fin observed at later stages of development (Fig. 1G-I).

Despite these conspicuous dorsal CNS defects, ventral CNS appears to neurulate normally, as suggested by the unaltered expression patterns of the floor plate marker *shh* (Krauss et al., 1993) and the basal plate marker *pax6* (Krauss et al., 1991) in

the 12-somite stage hindbrain (Fig. 4I,J). To locate the DV border between the ventral (morphologically unaffected) and dorsal domains, we analyzed the expression of *pax7*, identifying the basal/alar interface. *pax7* appears expressed in the dorsal-most cells of *pac* mutant neural tubes, suggesting that basal cells do converge to the midline, while alar cells remain excluded from this process. At least transiently, cavitated neural tube structures consisting solely of basal cells are formed (Fig. 2C; Fig. 4K-N), while alar neural cells remain in ectopic structures dorsal or lateral to the ventral 'neural tubes' (Fig. 4M,N). However, we failed to detect a morphological border between basal and alar structures at later

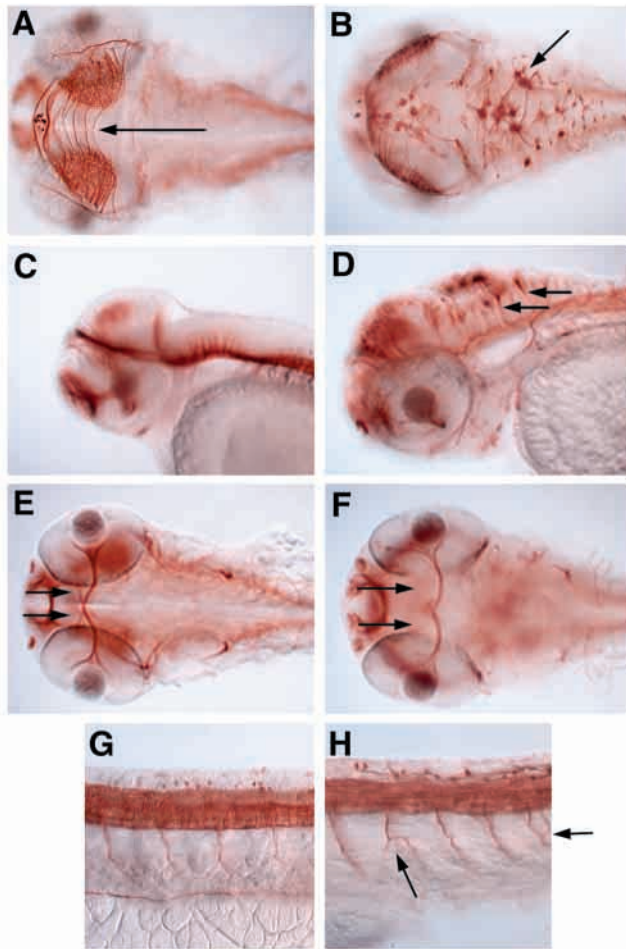


**Fig. 6.** Lack of *Ncad* leads to ectopic neurons in dorsal regions of mid-hindbrain and axonal projection defects. Anti-acetylated tubulin immunostaining in (A,C,E,G) wild type and (B,D,F,H) *pac*<sup>Jr7</sup> mutant; 60 hpf; dorsal/ventral views (A,B,E,F) and lateral view (C,D) of the head, and lateral view of the trunk anterior of the anus (G,H). (A-D) Arrow in A indicates tectal commissures missing in B. Arrows in B,D indicate large dorsal neurons projecting axons to each other (B) and ventrally (D). (E,F) Arrows indicate optic nerves crossing the midline in optic chiasma in E, but not in F. (G,H) Left arrow in H indicates branching intersomitic axon, right arrow indicates two converging axons from different motoneurons.

stages of development (Fig. 2B,C, and data not shown), suggesting that it might only be present transiently.

To test whether the apparently asymmetric neurulation phenotype along the DV axis of *pac* mutant neural tubes might be due to a differential requirement of *Ncad* for convergence of alar versus basal cells, we compared the neurulation behavior of wild-type and *pac* cells, co-transplanted into a region of wild-type host embryos giving rise to the basal plate. In all cases ( $n=10$ ), wild-type and mutant cells sorted out, resulting in neural tubes with the wild-type cells located basally, while *pac* cells were excluded from the basal plate, ending up in more dorsal regions of the alar plate (Fig. 4O,P; also see Fig. 2K). This suggests that *pac* mutant cells are compromised in their ability to move medially compared with their wild-type neighbors, even when they are initially positioned in territories close to the midline. Thus, *ncad*

appears to be cell-autonomously required for normal convergence behavior of both basal and alar neuroectodermal cells during neural tube morphogenesis.

### ***Ncad* controls neuronal localization in the mid- and hindbrain**

Although neurulation is affected in *pac* mutants, early stages of neurogenesis and neuronal specification proceed normally as evidenced, for example, by *ngn1* expression (DV patterning; not shown), or by *pax2.1* and *krox20* expression (AP patterning; Fig. 5A,B). However, subsequent to their birth, neurons frequently adopt inappropriate positions in the CNS of *pac* mutants (Fig. 5). Importantly, neuronal mis-positioning defects are observed along both the AP and the DV axes, and affect both alar and basal neurons – even though the basal plate is not significantly affected by the neurulation defects.

To examine neuronal patterning in the ventral CNS, we monitored the position of cranial motoneurons and reticulospinal neurons. Along the AP axis, *zcoe2*-positive (Bally-Cuif et al., 1998) motoneurons of the anterior hindbrain abnormally spread across the mid-hindbrain boundary (Fig. 5C,D). Similarly, the AP position of hindbrain interneurons appears randomized. Thus, *lim1*-positive interneurons (Toyama et al., 1995b) in *pac* mutants fail to reflect the rhombomeric organization of the hindbrain (Fig. 5E,F), while retrograde labeling reveals a randomization in the AP organization of all reticulospinal neurons (Fig. 5M-O). Most strikingly, individual *pac* mutant embryos display different reticulospinal patterns, as previously shown for the Mauthner neurons (Jiang et al., 1996) (highlighted on Fig. 5N,O). Furthermore, the mutant reticulospinal patterns lack bilateral symmetry, supporting the notion that the abnormal positioning of neurons in post-neurulation *pac* mutant neural tubes does not result from earlier patterning defects. Along the DV axis of *pac* mutant neural tubes, *phox2a*- (Fig. 5G,H) (Guo et al., 1999) and *isll*-positive hindbrain motoneurons (Fig. 5I,J) (Inoue et al., 1994) and *pax2.1*-positive hindbrain interneurons (Fig. 5K,L) (Mikkola et al., 1992) were all found in ectopic dorsal locations. In the spinal cord of *pac* mutants, by contrast, inappropriate positioning of neurons is less severe (Fig. 5K,L).

These data, together with the lack of AP or DV patterning defects during earlier stages of neural development in *pac* neural tubes, strongly suggest that *Ncad* is required to allow mid- and hindbrain neurons to reach or maintain their appropriate positions within the neural tube.

To directly address a potential role of *Ncad* in controlling neuronal motility within the embryonic CNS, we labeled single cells in the presumptive midbrain region of *pac* or wild-type embryos at an early gastrula stage, and determined the spatial distribution of their descendants at later stages of development. Although wild-type and *pac* mutant clones had similar cell numbers (wild type, 8 (5-12); *pac*, 9 (6-12)), *pac* mutant cells were spread over a significantly longer stretch along the AP and the DV axis than wild-type cells (Fig. 5P-R). Wild-type clones in average extended over eight (6-14) cell diameters along the AP axis and were all in one DV plane ( $n=10$ ), whereas *pac* mutant clones extended over 13 (9-20) cell diameters along the AP and over four (3-5) cell diameters along the DV axis ( $n=5$ ). Together, these data directly indicate that *Ncad* is generally required to restrict neuronal motility within the embryonic mid- and hindbrain, a property that might

account for the neuronal positioning defects detectable in *pac* mutants at post-neurulation stages.

### ***pac* mutants display supernumerary and ectopic neurons in dorsal regions of the midbrain and hindbrain**

Despite their mislocalization, most neuronal subtypes are generated in relatively normal numbers. However, selective neuronal populations appear over-represented. *lim1*-positive interneurons, for example, are found at high density in dorsal regions of midbrain and hindbrain of *pac* mutants at 24 hpf (Fig. 5E,F). Supernumerary and ectopic neurons in dorsal regions of the midbrain and hindbrain are also revealed by anti-acetylated tubulin immunohistochemistry at later stages. At 60 hpf, mutant embryos display acetylated tubulin-positive neurons in the tectum and dorsal hindbrain, while wild-type embryos of this stage are devoid of such cells (Fig. 6A-D). These large neurons, the identity of which is currently unknown as they proved negative for all identity markers tested, are often interconnected with each other by a network of axonal processes (Fig. 6B). A neural crest origin for these extra neurons can most likely be excluded because, as discussed below, neural crest cells form, migrate and differentiate normally in *pac*. The generation of these neurons might rather be linked to an hyperproliferation of dorsal neural cells in *pac* mutants (see below). Alternatively, defects in late steps of neural tube DV patterning, due, for example, to the absence of late dorsalizing signals generated by the altered *pac* roof plate, might account for this phenotype (Lee et al., 2000). Additional experiments will be necessary to resolve this issue.

### ***pac* is required for commissure formation in the forebrain and midbrain and peripheral axon pathfinding**

Although the most striking neural phenotypes occur in the midbrain and hindbrain of *pac* mutants, anti-acetylated tubulin immunohistochemistry revealed defects in axon pathway formation in other regions of the CNS and PNS. Optic axons exit the eye normally, but fail to form a normal commissure at the optic chiasm (Fig. 6E,F). Commissural pathfinding defects were also observed for Mauthner cell axons (data not shown) (Jiang et al., 1996), and in the formation of intertectal commissures (Fig. 6A,B). Finally, we observed defects in the axonal projections of spinal cord motoneurons, which normally run ventrally in the middle of each somite. In mutant embryos, these axons are sometimes divided into two branches (Fig. 6H). In addition, occasionally, axons ectopically exit the spinal cord, forming two ventral roots from a single spinal cord segment (Fig. 6H).

### **Defects in cell adhesion are associated with a destabilization of membrane-associated $\beta$ -catenin and an increased number of mitotic cells**

To determine whether the altered cell morphology in dorsal regions of the brain of *pac* mutants was associated with intracellular defects, we monitored cellular architecture with antibodies directed against cytoskeletal elements and associated proteins. As described, the cytoplasmic domain of Ncad binds  $\beta$ -catenin and other proteins of the cytoskeletal complex. Phalloidin staining and anti- $\alpha$ -tubulin immunocytochemistry, however, failed to reveal any gross

disorganization of the actin or tubulin cytoskeletal network in mutants (not shown). By contrast, the distribution of  $\beta$ -catenin is altered. We analyzed  $\beta$ -catenin localization at the 12-somite stage, shortly after *pac* mutants could be morphologically identified, but before the loss of integrity of dorsal neural tube cells. At this stage, anti- $\beta$ -catenin immunostaining of wild-type embryos revealed a DV gradient of membrane-associated (probably cadherin-bound)  $\beta$ -catenin, with highest levels in dorsal cells of the neural tube (Fig. 7A). In *pac* mutant embryos, dorsal neural tube cells appear very weakly stained compared with ventral cells (Fig. 7B). Thus, at the cellular level, Ncad appears to control the stabilization of the membrane-associated  $\beta$ -catenin complex in a regional manner along the DV axis of the neural tube.

In addition, dorsal neural tube cells of *pac* mutants display increased numbers of mitotically active cells, as revealed by immunostaining of phosphorylated histone 3 (phosphH3). Counting of phosphH3-positive cells in the region between the caudal limit of the optic lobes and the anterior limit of the otic vesicle at the 10- to 12-somite stage revealed significantly more cells in *pac* mutants than in their wild-type siblings (for *pac*<sup>fr7</sup> mutant, 12-somite stage: in average 163 cells/embryo, compared with 102 cells/embryo in wild type, five embryos each; for *pac*<sup>paR2.10</sup> mutant, 10-somite stage: in average 75 cells/embryo, compared with 56 cells/embryo in wild type, four embryos each). Thus, the number of mitotic cells in the neural tube of *pac* mutants is increased up to 1.6-fold. In addition, while phosphH3-positive cells are normally restricted to the ventricular zone of the neural tube (Fig. 7C,E), the position of these cells appears randomized in *pac* mutants (Fig. 7D). Sectioning further revealed that this randomization occurs only in the dorsal part of the neural tube, while ventrally mitotic cells are still restricted to the ventricular zone as in wild-type embryos (Fig. 7F). No obvious increase in the number of phosphH3-positive cells was observed at earlier or later segmentation stages, indicating that the effect of the *ncad* mutations on cell proliferation may be limited to a rather narrow time window of neural tube development.

## **DISCUSSION**

Ncad is one of the most thoroughly studied classical cadherins and several lines of in vitro evidence indicate roles in cell adhesion and migration. The importance of Ncad in early neural development has been inferred from its expression pattern and from embryonic manipulations. However, definitive evidence of its precise in vivo role(s) during vertebrate neural tube development has been lacking. Although defects in heart development, somitogenesis and establishment of left-right asymmetry of *Cdh2*<sup>-/-</sup> mice have been thoroughly analyzed (Radice et al., 1997), characterization of neural tube phenotypes has been limited (Luo et al., 2001). Here, we attempt to fill this void by providing a detailed analysis of the neural phenotype of the *ncad* zebrafish mutant *pac*. Our results highlight new and crucial roles of Ncad in the control of neural tube morphogenesis, maintenance of neural tube integrity, axonal pathfinding and neural cell proliferation, providing the first general description of the in vivo neuronal functions of Ncad.

### The truncated proteins encoded by *pac<sup>fr7</sup>* and *pac<sup>tm101B</sup>* are most likely functional nulls

Members of the classical cadherin subfamily have five extracellular (EC) domains mediating homophilic interactions between identical cadherins, while the intracellular, C-terminal part of the protein contains a binding domain for catenins that links the intramembranous cadherins to the actin cytoskeleton. The two *pac* alleles *pac<sup>fr7</sup>* and *pac<sup>tm101B</sup>* have a premature stop codon in the extracellular part of the protein, resulting in C-terminally truncated Ncad that lacks the extracellular domains EC4 and EC5, the transmembrane domain and the cytoplasmic region with its  $\beta$ -catenin-binding domain. These mutations should lead to the loss of both the intracellular and the intercellular functions of Ncad. It is likely that these truncated proteins are secreted. However, they might remain associated with the cell surface, perhaps through interactions of the remaining three N-terminal EC domains with other membrane proteins. We were not able to address this issue as none of the available anti-Ncad antibodies recognizes EC1-EC3. Nevertheless, two lines of evidence suggest that the remaining three EC domains of the truncated proteins encoded by *pac<sup>fr7</sup>* and *pac<sup>tm101B</sup>* lack most, if not all, of the crucial extracellular activities of wild-type Ncad, and do not perturb development in a dominant-negative fashion. First, recent data obtained in cell culture experiments point to a particularly important role for the EC4 domain in the regulation of cell adhesion and migration, and EC4 is missing in both truncated versions (Kim et al., 2000). Second, and most importantly, the *pac<sup>fr7</sup>* and *pac<sup>tm101B</sup>* alleles are recessive and as strong as *pac<sup>paR2.10</sup>*, which (according to our analysis) fails to generate any Ncad protein.

### Zebrafish *pac* phenotypes do not recapitulate all functions of Ncad known in other systems

As described, the *pac* phenotype is largely restricted to the embryonic neural tube. In vivo studies in other vertebrates, however, suggested roles for Ncad in controlling several developmental processes aside from neural tube development. For example, Ncad was proposed to control cell delamination and migration during chick neural crest formation (Nakagawa and Takeichi, 1998). The phenotype of *pac* mutants, however, does not support such a role in the zebrafish. Neural crest development does not seem affected in *pac* embryos. Pigmentation is normal and Alcian Blue staining did not reveal any differences in the number and morphological appearance of cartilagenous elements of the cranium (data not shown). Similarly, *pac* mutants, unlike *Ncad<sup>-/-</sup>* mice (Radice et al., 1997), did not suffer from obvious cardiac defects. In addition, no gross somite defects were apparent, and reversed heart laterality, observed in the chick upon incubation with blocking Ncad antibodies (Garcia-Castro et al., 2000), was found at equal rates in *pac* and wild-type embryos (not shown).

We can only speculate about why the phenotype of *pac* mutant embryos in non-neural tissues is less severe than that caused by Ncad deficiencies in other vertebrates. Partial complementation by maternally provided *ncad* gene products is unlikely, as no Ncad protein and no *ncad* mRNA could be detected in freshly laid eggs (see Fig. 3C). Other cadherins with an overlapping activity or expression pattern might compensate for the lack of Ncad in non-neural tissues. Such a partly redundant protein could be encoded by an *ncad* paralog

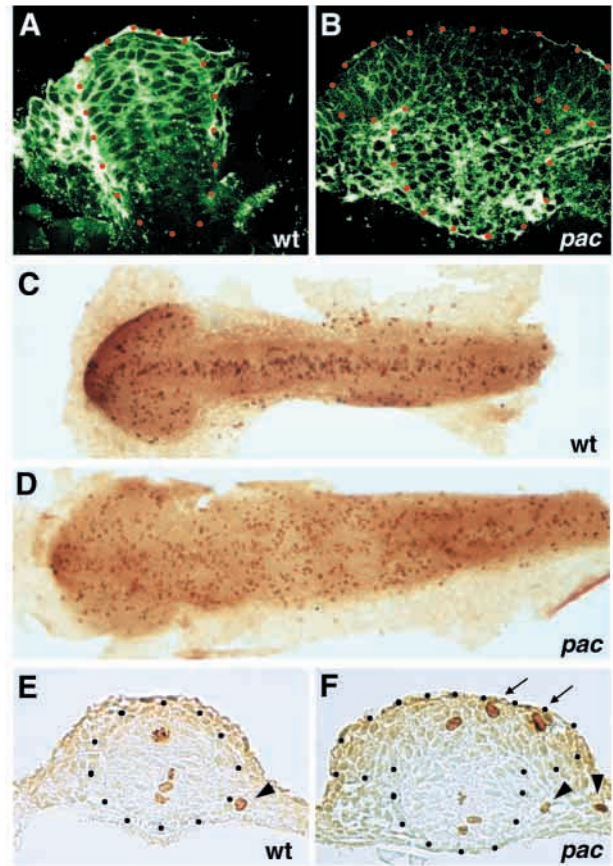


**Fig. 7.** *pac* mutants display loss of membrane-associated  $\beta$ -catenin and enhanced cell proliferation in dorsal regions of midbrain and hindbrain. (A,B) Anti- $\beta$  catenin immunostaining on 2  $\mu$ m confocal cross-sections through the hindbrain of wild-type (A) and *pac<sup>paR2.10</sup>* mutant sibling (B); 12-somite stage. (C-F) Anti-phosphH3 immunostaining of wild-type sibling (C,E) and *pac<sup>fr7</sup>* mutant (D,F) embryos of the 12-somite stage; flat mounts of whole embryos (C,D), and representative cross-sections at the hindbrain level (E,F). Mitotic cells in the lateralmost position (indicated by arrowheads) are not part of the neural tube and are probably migrating neural crest cells. In A,B,E,F, the neural tube is outlined by dots. Arrows in F point to ectopic phosphH3-positive cells in alar region of mutant.

generated during the genome duplication that is believed to have occurred during teleost evolution (Postlethwait et al., 2000). Alternatively, it could be encoded by a separate gene also found in other vertebrates, such as the so called *maternal N-cadherin* in *Xenopus*, which is clearly distinct in sequence from the 'regular' *Xenopus N-cadherin*, but shows a very similar zygotic expression pattern (Tashiro et al., 1995).

### Ncad regulates neuroectodermal cell adhesion

The phenotype of *pac* mutants demonstrates that Ncad is required to maintain neural tube integrity. In *pac* embryos, the classical pseudostratified neuroepithelium in the dorsal midbrain and hindbrain is lost, and cells instead delaminate and form cavitated cell aggregates. A role for Ncad in maintaining the integrity of the neuroepithelium was already postulated in the chick: in the neural tube of embryos treated with an anti-Ncad-specific antibody, aggregates called rosettes, which consist of a central ependymal lining surrounded by multiple

layers of differentiated neurons and glia, were formed (Gänzler-Odenthal and Redies, 1998). Our results provide a genetic confirmation of these data. Interestingly, the loss of neural tube integrity appears to be restricted to alar regions of *pac* mutants, whereas cells in basal regions appear morphologically normal. Along this line, it is noteworthy that R-cadherin has been described to be present in basal regions of the zebrafish mid- and hindbrain (Liu et al., 2001). This related molecule, or possibly other cadherins expressed in basal cells, might render them less dependent on Ncad function. A similar situation was described in the chick, where brain regions resistant to anti-Ncad antibody treatment were shown to express R-cadherin (Gänzler-Odenthal and Redies, 1998).

The defects of *pac* mutants in neural tube integrity might – directly or indirectly – result from the loss of Ncad function in mediating cell-cell adhesion. Studies in cell cultures have revealed both cell-adhesion enhancing and cell-adhesion inhibiting properties of Ncad, depending on the investigated cell types. Wild-type and *pac* neuroectodermal cells, when placed in a heterologous environment in chimeric neural tubes, display a typical exclusion behavior. In most cases, we observed that heterologous transplanted cells formed aggregates and did not integrate with their neighbors. This finding, in agreement with recent results obtained in chimeric mice (Kostetskii et al., 2001), directly identifies Ncad as a crucial component of neuroectodermal cell adhesivity in vivo. Because aggregates of wild-type cells in a *pac* environment are tighter than aggregates of *pac* cells in wild-type hosts, and because of the loose structure of the *pac* dorsal neural tube, we further propose that Ncad promotes adhesiveness of zebrafish neuroectodermal cells.

Our results do not allow us to conclude whether cell adhesiveness is differentially affected in alar versus basal regions of the neural tube. Isolated wild-type cells can normally integrate in the basal plate of *pac* mutants; however, this might simply reflect the ability of the cells to epithelialize. Epithelialization of neuroectodermal cells appears to occur rather independently of Ncad-mediated cell adhesion: although *pac* mutant cells fail to acquire a regular neuroepithelial shape in alar regions of wild-type host tubes, they can do so both in basal and – as rosettes – in alar regions of the neural tube of non-chimeric mutants.

In contrast to epithelialization, other cellular processes do seem affected by the altered adhesiveness of Ncad-deficient neuroectodermal cells. These include the convergence of neuroectodermal cells during neurulation, and the maintenance of neuronal positioning within the neural tube, discussed in the following two sections.

### Ncad regulates neurulation

Although a function of Ncad during neurulation had already been proposed by Hatta and Teikeichi (Hatta and Teikeichi, 1986), genetic data supporting this notion has so far been missing. In zebrafish, unlike in mammals, birds and amphibia, neurulation does not involve the invagination of an epithelial sheet, but the convergence of neuroectodermal cells towards the midline, secondarily followed by cavitation to form the neurocoel (Kimmel et al., 1995). As in other vertebrates, though, cells from medial regions of the neuroectoderm end up in ventral/basal regions of the neural tube, and cells from

lateral regions in dorsal/alar regions (Papan and Campos-Ortega, 1994). The mushroom-like shape of *pac* neural tubes and the altered expression patterns of various marker genes can be best interpreted by a delayed convergence of neuroectodermal cells in *pac* mutant embryos. This notion is strongly supported by data we obtained when directly comparing the neurulation behavior of wild-type and *ncad* mutant cells in co-transplantation studies. These studies revealed that the convergence capabilities of Ncad-deficient cells are compromised, as they sort-out to more lateral positions than wild-type cells during the neurulation process. The convergent extension movements underlying zebrafish neurulation are in part driven by medial cell intercalations (Warga and Kimmel, 1990), and should therefore require a tight and coordinated regulation of cell adhesiveness and motility. Ncad might be required for either of these properties, or both.

As for neural tube integrity, the convergence phenotype of *pac* neural tubes appears asymmetrical, being prominent in the alar domain while basal plate cells organize into a tube-like structure. This asymmetry might reflect a differential (direct or indirect) requirement for Ncad for the convergence abilities of alar versus basal cells. However, our observation that *pac* mutant cells display compromised convergence capability, even when co-transplanted to the basal plate, argues against this interpretation. Thus, the strong convergence phenotype of the alar plate in *pac* mutants is more likely to reflect the location of presumptive alar cells further away from the midline, while basal cells have to converge over a shorter distance. Along these lines, one might wonder why a transient but sharp transition in *pac* mutant neural tube morphology develops at the basal-alar interface, as reflected by the expression pattern of *pax7* outlining a basal ‘pseudo-tube’-like structure. In addition to basally expressed cadherins such as R-cadherin, mentioned previously, a candidate cadherin which might account for this sharp switch in cell behavior is F-cadherin. *Xenopus* F-cadherin is expressed at the border of the basal and alar plates, leads to impaired dorsal convergence upon overexpression, and is believed to regulate the positioning of neurons specifically in this region of the neural tube (Espeseth et al., 1998). Confirmation of this hypothesis awaits the molecular and functional characterization of zebrafish F-cadherin.

### Ncad regulates the positioning of postmitotic neurons within the neuroepithelium

A second unprecedented role for Ncad, possibly also resulting from its impact on cell-cell adhesion, is its involvement in controlling the positioning of probably all neuronal populations along the AP and DV axes of the midbrain and hindbrain. Some of these mislocalizations can be related to the impaired convergence of the alar plate (such as the more lateral positions of *isl1*-positive sensory neurons), while others can not (such as the AP and DV shifts of motor neurons in the basal plate). We demonstrate that these mislocalizations are not anticipated by AP and DV patterning defects at earlier stages of neurogenesis, and are more difficult to interpret in patterning terms because they often lack bilateral symmetry. Thus, they more likely result from unrestricted motility of neurons within the neural tube, following their initially normal specification. Indeed, our clonal analyses directly show that neurons in *pac*

mutant neural tubes do, on average, spread twice as far as in wild-type tubes. The neuronal mixing in *ncad* mutant embryos might be further enhanced by defective border formation and regionalization within the embryonic brain. Although we have not directly addressed this point, it might explain why hindbrain motoneurons and interneurons can move across the rhombomeric borders in the hindbrain of *ncad*-deficient embryos.

A role for cadherins in restricting neuronal mixing and creating boundaries has previously been described for cadherins with spatially restricted expression patterns within the CNS, such as for R-cadherin and cadherin 6 in prosencephalic domains in mouse (Inoue et al., 2001; McCarthy et al., 2001), and for F-cadherin at the basal-alar interphase in *Xenopus* (Espeseth et al., 1998). However, in contrast to these cadherins, zebrafish *ncad* displays ubiquitous expression throughout the CNS. Thus, the phenotype of *pac* mutants indicates that in addition to region-specific cadherins, general Ncad-mediated homophilic cell adhesion is necessary to restrict neuronal cell mixing and to maintain the pattern of neuronal specification established at early embryonic stages.

### The role of Ncad during axonogenesis

Embryological work in vertebrates, and recent genetic studies in *Drosophila* and *C. elegans* have revealed essential roles of Ncad proteins during axonal outgrowth and fasciculation in motoneurons (Broadbent and Pettitt, 2002; Iwai et al., 1997) and retinal cells of the visual system (Lee et al., 2001; Riehl et al., 1996; Stone and Sakaguchi, 1996). Similarly, *pac* zebrafish mutants display defects in the projection of motoneuron axons, and in commissure formation of optic and tectal axons. It remains unclear whether these defects of *pac* mutants reflect a primary role of Ncad in axonal pathfinding, or whether they are indirect consequences of a general perturbation of axonal cues due to incomplete neurulation or the loss of neural tube integrity. Thus, defective tectal commissure formation in *pac* mutants might be a secondary consequence of the early neurulation defects in this region of the brain, revealed by *emx1* and *wnt1* expression. However, some spinal cord motoneurons display irregular axon branching outside the neural tube in intersomitic trunk areas, which themselves lack *ncad* expression (see Fig. 3F), and which do not seem to be affected by the *pac* mutation. Thus, here, the abnormal axonal behavior is likely to be due to a cell-autonomous effect of the *pac* mutation in the projecting motoneuron. Chimeric analyses will be necessary to confirm this interpretation.

### Ncad has a negative effect on cell proliferation in the dorsal neural tube: a possible link to $\beta$ -catenin?

Finally, an additional striking phenotype of *pac* mutants was the hyperproliferation of alar regions of the neural tube during midsegmentation stages. Hyperproliferation occurs over a narrow time window, when the integrity of the alar region of the neural tube is intact. Therefore, it might not be a secondary effect of rosette formation, as previously described in Ncad-blocked chicken brains (Gänzler-Odenthal and Redies, 1998). Although highly speculative, the hyperproliferation in *pac* mutants might be linked to the shifts in  $\beta$ -catenin levels observed across the neural tube at the same developmental

stages. Activating  $\beta$ -catenin mutations have been implicated in cell overproliferation in numerous tumors, including medulloblastoma, a brain tumor affecting young children (Zurawel et al., 1998). *pac* mutant embryos show a decrease in the levels of membrane-associated  $\beta$ -catenin in dorsal cells, most likely as a result of the loss of Ncad protein as one of the  $\beta$ -catenin binding partners. This might lead to a temporary increase in the cytosolic and nuclear  $\beta$ -catenin pools, promoting cell proliferation. In light of these results, it is tempting to speculate that Ncad, by withdrawing  $\beta$ -catenin from the cytoplasmic pool, might help to regulate cell proliferation in the developing neural tube.

We thank Y.-J. Jiang for stimulating discussions and sharing unpublished results, and B. Geiger, C. Thisse, A. Fjose, P. Ingham, J. Odenthal, S. Guo, H. Okamoto and U. Strähle for providing us with plasmids and reagents. Work in M.H.'s laboratory was supported by the Max-Planck Society and HFSP (RG0354/1999-M); work in L. B.-C.'s laboratory was supported by a Junior Research Group grant of the Volkswagen Stiftung; work in S. W.'s laboratory was supported by the Wellcome Trust and BBSRC; work on F.R.'s laboratory was supported by the ARC, AFM and ACI; and work in R.G.'s laboratory was supported by the Max-Planck society and the German Human Genome Project (DHGP Grant 01 KW 9919). Z. L. thanks EMBO for his long-term postdoctoral fellowship. We are very grateful to T. Mayr, J. Buchholz and all members of F.R.'s laboratory for their participation in the mutant screens; to R. Ray for his help during the mapping of *pac*; and to J. Beer, S. Geiger-Rudolph and L. Saint-Etienne for excellent technical assistance. We also acknowledge other members of our laboratories for their critical contribution during the process of this work.

## REFERENCES

- Bally-Cuif, L., Dubois, L. and Vincent, A. (1998). Molecular cloning of *zco2*, the zebrafish homolog of *Xenopus Xco2* and mouse *EBF-2*, and its expression during primary neurogenesis. *Mech. Dev.* **77**, 85-90.
- Bally-Cuif, L., Goutel, C., Wassef, M., Wurst, W. and Rosa, F. (2000). Coregulation of anterior and posterior mesoderm development by a hairy-related transcriptional repressor. *Genes Dev.* **14**, 1664-1677.
- Bitzur, S., Kam, U. and Geiger, B. (1994). Structure and disruption of N-cadherin in developing zebrafish embryos: morphogenetic effects of ectopic over-expression. *Dev. Dyn.* **201**, 121-136.
- Broadbent, I. E. and Pettitt, J. (2002). The *C. elegans* *hmr-1* gene can encode a neuronal classic cadherin involved in the regulation of axon fasciculation. *Curr. Biol.* **12**, 59-63.
- Dickmeis, T., Mourrain, P., Saint-Etienne, L., Fischer, N., Anstadt, P., Clark, M., Strähle, U. and Rosa, F. (2001). Casanova, a gene crucial for endoderm development, encodes a novel sox-related molecule. *Genes Dev.* **15**, 1487-1492.
- Dufour, S., Beauvais-Jouneau, A., Delouvé, A. and Thiery, J. P. (1999). Differential function of N-cadherin and Cadherin-7 in the control of embryonic cell motility. *J. Cell Biol.* **146**, 501-516.
- Espeseth, A., Marnellos, G. and Kintner, C. (1998). The role of *F-cadherin* in localizing cells during neural tube formation in *Xenopus* embryos. *Development* **125**, 301-312.
- Gänzler-Odenthal, S. I. I. and Redies, C. (1998). Blocking N-cadherin function disrupts the epithelial structure of differentiating neural tissue in the embryonic chicken brain. *J. Neurosci.* **18**, 5415-5425.
- Garcia-Castro, M. I., Vielmetter, E. and Bronner-Fraser, M. (2000). N-cadherin, a cell adhesion molecule involved in establishment of embryonic left-right asymmetry. *Science* **288**, 1047-1051.
- Guo, S., Brush, J., Teraoka, H., Goddard, A., Wilson, S. W., Mullins, M. C. and Rosenthal, A. (1999). Development of noradrenergic neurons in the zebrafish hindbrain requires BMP, FGF8, and the homeodomain protein *souless/Phox2a*. *Neuron* **24**, 555-566.
- Hammerschmidt, M., Pelegri, F., Mullins, M. C., Kane, D. A., van Eeden, F. J. M., Granato, M., Brand, M., Furutani-Seiki, M., Hafter, P.,

- Heisenberg, C.-P. et al. (1996). *dino* and *mercedes*, two genes regulating dorsal development in the zebrafish embryo. *Development* **123**, 95-102.
- Hatta, K. and Takeichi, M. (1986). Expression of N-cadherin adhesion molecules associated with early morphogenetic events in chick development. *Nature* **320**, 447-449.
- Hazan, R. B., Phillips, G. R., Qiao, R. F., Norton, L. and Aaronson, S. A. (2000). Exogenous expression of N-cadherin in breast cancer cells induces cell migration, invasion and metastasis. *J. Cell Biol.* **148**, 779-790.
- Ho, R. K. and Kane, D. A. (1990). Cell-autonomous action of zebrafish *spt-1* mutation in specific mesodermal precursors. *Nature* **348**, 728-730.
- Inoue, A., Takahashi, M., Hatta, K., Hotta, Y. and Okamoto, H. (1994). Developmental regulation of *islet-1* mRNA expression during neuronal differentiation in embryonic zebrafish. *Dev. Dyn.* **199**, 1-11.
- Inoue, T., Tanaka, T., Takeichi, M., Chisaka, O., Nakamura, S. and Osumi, N. (2001). Role of cadherins in maintaining the compartment boundary between the cortex and striatum during development. *Development* **128**, 561-569.
- Islam, S., Carey, T. E., Wolf, G. T., Wheelock, M. J. and Johnson, K. R. (1996). Expression of N-cadherin by human squamous carcinoma cells induces a scattered fibroblastic phenotype with disrupted cell-cell adhesion. *J. Cell Biol.* **135**, 1643-1654.
- Iwai, Y., Usui, T., Hirano, S., Steward, R., Takeichi, M. and Uemura, T. (1997). Axon patterning requires DN-cadherin, a novel neuronal adhesion receptor, in the *Drosophila* embryonic CNS. *Neuron* **19**, 77-89.
- Jiang, Y.-J., Brand, M., Heisenberg, C.-P., Beuchle, D., Furutani-Seiki, M., Kelsh, R. N., Warga, R. M., Granato, M., Haffter, P., Hammerschmidt, M. et al. (1996). Mutations affecting neurogenesis and brain morphology in the zebrafish, *Danio rerio*. *Development* **123**, 205-216.
- Kelly, G. M. and Moon, R. T. (1995). Involvement of Wnt1 and Pax2 in the formation of the midbrain-hindbrain boundary in the zebrafish gastrula. *Dev. Genet.* **17**, 129-140.
- Kim, J.-B., Islam, S., Kim, Y. J., Prudoff, R. S., Sass, K. M., Wheelock, M. J. and Johnson, K. R. (2000). N-cadherin extracellular repeat 4 mediates epithelial to mesenchymal transition and increased motility. *J. Cell Biol.* **151**, 1193-1205.
- Kimmel, C. B., Ballard, W. W., Kimmel, S. R., Ullmann, B. and Schilling, T. F. (1995). Stages of embryonic development of the zebrafish. *Dev. Dyn.* **203**, 253-310.
- Knapik, E. W., Goodman, A., Atkinson, O., Roberts, C. T., Shiozawa, M., Sim, C. U., Weksler-Zangen, S., Trolliet, M. R., Futrell, C., Innes, B. A. et al. (1996). A reference cross DNA panel for zebrafish (*Danio rerio*) anchored with simple sequence length polymorphisms. *Development* **123**, 451-460.
- Kostetskii, I., Moore, R., Kemler, R. and Radice, G. L. (2001). Differential adhesion leads to segregation and exclusion of N-cadherin-deficient cells in chimeric embryos. *Dev. Biol.* **234**, 72-79.
- Krauss, S., Johansen, T., Korzh, V., Moens, U., Ericson, J. U. and Fjose, A. (1991). Zebrafish *pax[zf-a]*: a paired box-containing gene expressed in the neural tube. *EMBO J.* **10**, 3609-3619.
- Krauss, S., Korzh, V., Fjose, A. and Johansen, T. (1992). Expression of four zebrafish *wnt*-related genes during embryogenesis. *Development* **116**, 249-259.
- Krauss, S., Concordet, J.-P. and Ingham, P. W. (1993). A functionally conserved homolog of the *Drosophila* segment polarity gene *hh* is expressed in tissues with polarizing activity in zebrafish embryos. *Cell* **75**, 1431-1444.
- Lee, C. H., Herman, T., Clandinin, T. R., Lee, R. and Zipursky, S. L. (2001). N-cadherin regulates target specificity in the *Drosophila* visual system. *Neuron* **30**, 437-450.
- Lee, K. J., Dietrich, P. and Jessell, T. M. (2000). Genetic ablation reveals that the roof plate is essential for dorsal interneuron specification. *Nature* **403**, 734-740.
- Linask, K. K., Ludwig, C., Han, M.-D., Liu, X., Radice, G. L. and Knudsen, K. (1998). N-cadherin/catenin-mediated morphoregulation of somite formation. *Dev. Biol.* **202**, 85-102.
- Liu, Q., Marrs, J. A., Chuang, J. C. and Raymond, P. A. (2001). Cadherin-4 expression in the zebrafish central nervous system and regulation by ventral midline signaling. *Dev. Brain Res.* **131**, 17-29.
- Luo, M., Ferreira-Cornwell, C., Baldwin, H. S., Kostetskii, I., Lenox, J. M., Lieberman, M. and Radice, G. L. (2001). Rescuing the N-cadherin knockout by cardiac-specific expression of N- or E-cadherin. *Development* **128**, 459-469.
- McCarthy, M., Na, E., Neyt, C., Langston, A. and Fishell, G. (2001). Calcium-dependent adhesion is necessary for maintenance of prosomeres. *Dev. Biol.* **233**, 80-94.
- Mikkola, I., Fjose, A., Kuwada, J. Y., Wilson, S., Guddal, P. H. and Krauss, S. (1992). The paired domain-containing nuclear factor *pax[b]* is expressed in specific commissural interneurons in zebrafish embryos. *J. Neurobiol.* **23**, 933-946.
- Miyatani, S., Shimamura, K., Hatta, M., Nagafuchi, A., Nose, A., Matsunaga, M., Hatta, K. and Takeichi, M. (1989). Neural cadherin: Role in selective cell-cell adhesion. *Science* **245**, 631-635.
- Moens, C. B., Yan, Y.-L., Appel, B., Force, A. G. and Kimmel, C. B. (1996). *Valentino*: a zebrafish gene required for normal hindbrain segmentation. *Development* **122**, 3981-3990.
- Morita, T., Nitta, H., Kiyama, Y., Mori, H. and Mishina, M. (1995). Differential expression of two zebrafish *emx* homeoprotein mRNAs in the developing brain. *Neurosci. Lett.* **198**, 131-134.
- Nakagawa, S. and Takeichi, M. (1998). Neural crest emigration from the neural tube depends on regulated cadherin expression. *Development* **125**, 2963-2971.
- Nasevicius, A. and Ekker, S. C. (2000). Effective targeted gene 'knockdown' in zebrafish. *Nat. Genet.* **26**, 216-220.
- Nieman, M. T., Prudoff, R. S., Johnson, K. R. and Wheelock, M. J. (1999). N-cadherin promotes motility in human breast cancer cells regardless of their E-cadherin expression. *J. Cell Biol.* **147**, 631-643.
- Odenthal, J. and Nüsslein-Volhard, C. (1998). *forkhead domain* genes in zebrafish. *Genes Dev. Evol.* **208**, 245-258.
- Papan, C. and Campos-Ortega, J. (1994). On the formation of the neural keel and neural tube in the zebrafish *Danio rerio*. *Roux's Arch. Dev. Biol.* **203**, 178-186.
- Postlethwait, J. H., Woods, I. G., Ngo-Hazelett, P., Yan, Y.-L., Kelly, P. D., Chu, F., Huang, H., Hill-Force, A. and Talbot, W. S. (2000). Zebrafish comparative genomics and the origins of vertebrate chromosomes. *Genome Res.* **10**, 1890-9051.
- Radice, G. L., Rayburn, H., Matsunami, H., Knudsen, K. A., Takeichi, M. and Hynes, R. O. (1997). Developmental defects in mouse embryos lacking N-cadherin. *Dev. Biol.* **181**, 64-78.
- Rauch, G.-J., Granato, M. and Haffter, P. (1997). A polymorphic zebrafish line for genetic mapping using SSLPs on high-percentage agarose gels. *Tech. Tips Online* T01208.
- Redies, C. (2000). Cadherins in the central nervous system. *Prog. Neurobiol.* **61**, 611-648.
- Redies, C. and Takeichi, M. (1993). Expression of N-cadherin mRNA during development of the mouse brain. *Dev. Dyn.* **197**, 26-39.
- Redies, C., Engelhardt, K. and Takeichi, M. (1993). Differential expression of N- and R-cadherin in functional neuronal systems and other structures of the developing chicken brain. *J. Comp. Neurol.* **333**, 398-416.
- Riehl, R., Johnson, K., Bradley, R., Grunwald, G. B., Cornel, E., Lilienbaum, A. and Holt, C. E. (1996). Cadherin function is required for axon outgrowth in retinal ganglion cells in vivo. *Neuron* **17**, 837-848.
- Schnadelbach, O., Blaschuk, O. W., Symonds, M., Gour, B. J., Doherty, P. and Fawcett, J. W. (2000). N-cadherin influences migration of oligodendrocytes on astrocyte monolayers. *Mol. Cell. Neurosci.* **15**, 288-302.
- Serbedzija, G. N., Chen, J.-N. and Fishman, M. (1998). Regulation in the heart field of zebrafish. *Development* **125**, 1095-1101.
- Stone, K. E. and Sakaguchi, D. S. (1996). Perturbation of the developing *Xenopus* retinotectal projection following injections of antibodies against beta1 integrin receptors and N-cadherin. *Dev. Biol.* **180**, 297-310.
- Tashiro, K., Tooi, O., Nakamura, H., Koga, C., Ito, Y., Hikasa, H. and Shiokawa, K. (1995). Cloning and expression studies of cDNA for a novel *Xenopus* cadherin (XmN-cadherin), expressed maternally and later neural-specifically in embryogenesis. *Mech. Dev.* **54**, 161-171.
- Tepass, U., Truong, K., Godt, T., Ikura, M. and Peifer, N. (2000). Cadherins in embryonic and neural morphogenesis. *Nat. Rev. Mol. Cell. Biol.* **1**, 91-100.
- Thisse, C., Thisse, B. and Postlethwait, J. H. (1995). Expression of *snail2*, a second member of the zebrafish *snail* family, in cephalic mesoderm and presumptive neural crest of wild-type and *spadetail* mutant embryos. *Dev. Biol.* **172**, 86-99.
- Toyama, R., Curtiss, P. E., Otani, H., Kimura, M., Dawid, I. B. and Taira, M. (1995a). The LIM class homeobox gene *lim-5*: implied role in CNS patterning in *Xenopus* and Zebrafish. *Dev. Biol.* **170**, 583-593.
- Toyama, R., O'Connell, M. C., Wright, C. V. E., Kuehn, M. R. and Dawid, I. B. (1995b). *nodal* induces ectopic *gooseoid* and *lim1* expression and axis duplication in zebrafish. *Development* **121**, 383-391.
- Tran, N. L., Nagle, R. B., Cress, A. E. and Heimark, R. L. (1999). N-cadherin expression in human prostate carcinoma cell lines. An epithelial-

- mesenchymal transformation mediating adhesion with stromal cells. *Am. J. Pathol.* **155**, 787-798.
- Warga, R. M. and Kimmel, C. B.** (1990). Cell movements during epiboly and gastrulation in zebrafish. *Development* **108**, 569-580.
- Woo, K. and Fraser, S. E.** (1995). Order and coherence of the fate map of the zebrafish nervous system. *Development* **121**, 2595-2609.
- Yagi, T. and Takeichi, M.** (2000). Cadherin superfamily genes: functions, genomic organization, and neurologic diversity. *Genes Dev.* **14**, 1169-1180.
- Zurawel, R. H., Chiappa, S. A., Allen, C. and Raffel, C.** (1998). Sporadic medulloblastoma contain oncogenic beta-catenin mutations. *Cancer Res.* **58**, 896-899.